11176-H298-RO-00

PROJECT TECHNICAL REPORT

APOLLO 9
LM-3
ASCENT PROPULSION SYSTEM
FINAL FLIGHT EVALUATION

NAS 9-8166

July 1969

Prepared for
NATIONAL AERONAUTICS AND SPACE ADMINISTRATION
MANNED SPACECRAFT CENTER
HOUSTON, TEXAS

TRW
SYSTEMS GROUP

N 70-34530

11176-H298-RO-00

PROJECT TECHNICAL REPORT

APOLLO 9
LM-3
ASCENT PROPULSION SYSTEM
FINAL FLIGHT EVALUATION

NAS 9-8166

July 1969

Prepared for
NATIONAL AERONAUTICS AND SPACE ADMINISTRATION
MANNED SPACECRAFT CENTER
HOUSTON, TEXAS

Prepared by
P. F. Thompson
W. G. Griffin
Members of the Technical Staff
Propulsion Technology Section
Power Systems Department

Approved by: P. H. Janak
P. H. Janak, Head
Propulsion Technology Section

Approved by: P. H. Janak for D. W. Vernon
D. W. Vernon, Manager
Power Systems Department

Approved by: R. J. Smith
R. J. Smith, Manager
Task E-19E

TRW
SYSTEMS GROUP

ACKNOWLEDGMENTS

This document is a result of an integrated NASA Manned Spacecraft Center and TRW Systems effort. The authors wish to acknowledge the following individuals who made significant contributions to the analysis:

Joe Fries, NASA, for supervising the flight data processing and assisting in the flight data analysis;

John Hooper, NASA, for his assistance in analyzing the flight data and coordinating the postflight effort;

Warren Brasher, NASA, for the engine transient analysis.

CONTENTS

CONTENTS (Continued)

ILLUSTRATIONS

CONTENTS (Continued)

ILLUSTRATIONS

PURPOSE AND SCOPE

The purpose of this report is to present the results of the analysis of the Ascent Propulsion System (APS) performance during the Apollo 9 mission. The primary objective of this analysis was to determine the steady-state performance of the APS during the LM-3 Apollo 9 mission Burn to Depletion (BTD).

This report covers the additional analysis performed following the issuance of Reference 1, and the results herein supersede those contained in it.

The following items are the major additions to, or changes from the results issued in Reference 1:

1. The steady state performance values during the APS BTD are revised.
2. The analysis techniques, problems and assumptions are presented.
3. The residual errors (measured parameters minus program calculated) are presented.
4. The flight regulator anomaly is discussed in greater detail.
5. The engine throat erosion rate is presented.

SUMMARY

The Ascent Propulsion System (APS) was used for two firings; a 2.9 second firing while the ascent stage was manned and an unmanned firing to propellant depletion.

The 2.9 second manned burn occurred at a ground elapsed time (GET) of 96:58:14 (hours:minutes:seconds) and the unmanned burn to propellant depletion (BTD) began at 101:53:15.4. The Lunar Module (LM) was out of ground tracking station range during the first APS burn, therefore, no data from the burn were available. System pressures and temperatures were nominal when data was acquired after the burn. The second APS burn was initiated at 101:53:15.4 GET and the engine off signal was received at 101:59:17.7 GET, for a total duration of 362.3 seconds. During the second burn, system pressures were lower than nominal, indicating a malfunction in the Class I leg of the helium regulator package. The Class II primary helium regulator controlled helium flowrate during most of the burn. This is a planned mode of redundant operation, and the lower operating pressures produced no undesirable effects in the system. The second APS burn was terminated by the planned oxidizer-first propellant depletion. The oxidizer depletion occurred approximately 3 seconds early based on reconstructed flight performance and low level sensor data. The cause of this premature depletion was attributed to propellant sloshing as noted in the discussion. The rest of the depletion appeared nominal in all respects. The engine was commanded off at 101:59:17.7 GET.

The time integrated average engine specific impulse and average engine mixture ratio determined by ~~the~~ burn to depletion ~~(BTD)~~ analysis were 309.7 seconds and 1.601 respectively. Analysis of the flight data also indicated

that the APS engine throat erosion during the BTD was much greater than predicted. The expected LM-3 APS throat erosion at the termination of the BTD was approximately zero, while the erosion calculated from LM-3 flight data for the same time was approximately 5%. This higher erosion rate will be investigated in more detail and future flight data will be reviewed for evidence of this phenomena.

INTRODUCTION

The Apollo 9 mission was the ninth in a series of flights using specification Apollo hardware and the first manned flight of the Lunar Module. This mission was the third manned flight of Block II Command and Service Modules and the second manned flight using a Saturn V launch vehicle. The mission was a 10-day flight to qualify the Lunar Module and to demonstrate certain spacecraft functions for manned lunar flight.

Launch occurred at 11:00 A.M. (EST) on March 3, 1969, with the Apollo 9 spacecraft being initially inserted into an earth orbit of 102.3 by 103.9 nautical miles. After the post-insertion checkout was completed, the Command and Service Modules were separated from the S-IVB, transposed and docked with the Lunar Module.

One firing of the descent engine and five service propulsion firings were performed while the spacecraft were in the docked configuration.

Two crewmen transferred to the Lunar Module at about 89 hours to perform a Lunar-Module-Active Rendezvous. The Descent Propulsion System was used to perform the phasing and insertion maneuvers and the Ascent Propulsion System was fired for 2.9 seconds to establish a constant differential height after the coelliptic sequence had been initiated. The rendezvous and docking were completed satisfactorily. The ascent stage was jettisoned 2.5 hours later and a separation maneuver was performed by the Command and Service Module. The ascent stage was ignited at 101:53:15 GET for a 362.3 second firing of the ascent engine to oxidizer first propellant depletion. Ignition and cutoff times plus velocity change data are shown in Table 1.

The Apollo 9 LM-3 Ascent Propulsion System (APS) was equipped with Rocketdyne Engine S/N 0004B. The LM-3 APS engine performance was derived based on characterization equations from Reference 4, engine data from Reference 3 and flight measurement data. The engine and feed system physical characteristics are presented in Table 2.

The LM-3 APS analysis consisted of investigation of the engine steady-state performance and transient performance during the BTD, propellant utilization, and ullage pressurization system characteristics. These items are discussed in detail in this report.

STEADY-STATE PERFORMANCE ANALYSIS

Analysis Technique

The Ascent Propulsion System (APS) performance analysis was primarily concerned with determining the steady-state performance during the 2nd ascent engine firing, which was the burn to oxidizer first propellant depletion.

During the first ascent engine firing (CDH burn), the Lunar Module was out of ground-tracking-station range, therefore, no data was available.

The analysis of the BTD used the following flight measurement data: chamber pressure, engine interface pressures, tank bottom to engine interface delta pressures, vehicle thrust acceleration, propellant tank bulk and interface temperatures, helium regulator outlet pressures, propellant low level sensor uncover times, engine on-off commands and RCS thruster solenoid bi-level measurements. Measurement numbers and other data pertinent to the above measurements are given in Table 3 while the measured data is presented in the Appendix. The analysis of the APS was performed with the aid of the Apollo Propulsion Analysis Program. This program utilizes a minimum variance technique to establish the best correlation between the available ground and flight test data. The program uses error models of the available data as inputs plus a non-linear APS simulation model and by iteration establishes a "best" estimate (minimum variance of the available data) of the system performance history, propellant weights, and lunar module damp weight.

Analysis Program Results

The ascent engine BTD duty cycle consisted of a burn of 362.3 seconds duration which was initiated successfully at 101:53:15.4 GET and terminated (engine cutoff signal) at 101:59:17.7 GET. The portion of the APS BTD which was analyzed to determine steady-state performance included the time from 101:53:30 to 101:57:30 GET. This covered the period of the burn from approximately 15 seconds after ignition, eliminating the start transient effects, to the time 15 sec prior to when the system pressures increased due to the helium regulator returning to nominal operating level.

The results of the APS BTD steady-state analysis are as follows:

1) The ascent engine throat area eroded 5.3% during the BTD. (Figure 1)

2) The integrated time average ascent engine specific impulse during the BTD was 309.7 seconds. The specific impulse during the 240 seconds of the steady-state analysis is presented in Figure 2.

3) The average engine mixture ratio was 1.601 based on low level sensor actuation times.

4) A helium regulator malfunction (Section 6) caused low system operating pressures.

5) The APS BTD appeared nominal except for items 1 and 4 above.

The APS BTD analysis results are presented in Figures 1 - 19. The plots contain flight data, residual errors (difference between flight data and program calculated values) program calculated parameters, and preflight comparisons. The figures include engine chamber pressure, oxidizer interface pressure, fuel interface pressure, acceleration, oxidizer and fuel differential pressure (propellant tank bottom to engine interface), specific impulse, thrust, engine oxidizer and fuel flowrates, throat erosion and RCS performance.

Discussion

During the BTD there were two exceptions to expected performance: lower system operating pressures and increasing differential (delta) pressures (propellant tank bottom to engine interface). The lower system operating pressures resulted from the helium regulator malfunction, as noted in the helium regulator performance section, and were simulated in the APS model with measured engine interface pressure (oxidizer and fuel). Nominally the differential pressures are decreasing; therefore, the increasing differential pressures trend was investigated. The analysis of the flight performance indicated that the degree of throat erosion experienced during the BTD was much greater than predicted and of such a magnitude to cause the noted differential pressures.

In order to verify the increasing differential pressure trend an investigation was made to determine the validity of the measurements and reasons for this phenomenon. There were three items uncovered which affected these measurements.

1) The measurements on the cold flow test were not in exactly the same location as the flight measurements and, therefore, the feed line resistances accompanying these measurements required recalculation to be consistent with the flight measurement locations.

2) It was found that the effect on the differential pressure measurements of flow through the APS interconnect to the RCS was appreciable, requiring it to be more accurately assessed.

3) It was noted that the differential pressure transducer lines were not bled after propellant loading, and therefore, gas was trapped

in the transducer lines. The system was then brought to flight pressures and gas was still displacing the liquid in the transducer lines,thus presenting erroneous differential pressure readings. The gas in the lines did not cancel out the head effect of the liquid in the propellant feed lines. Therefore, the pressure trend indicated a greater differential pressure increase than was actually occuring. This trend manifested itself on the reconstruction as an indication of an even greater throat erosion than was actually experienced.

The above three items were modeled into the APS simulation incorporating all the available data, and the predicted throat erosion rate. The flight data still could not be satisfactorily simulated. The simulation deviated in the areas of tank bottom to engine interface differential pressures, chamber pressure and acceleration. To achieve a satisfactory residual match (measurement data minus calculated data), higher flowrates and thrust were indicated. In an attempt to simulate the increased flowrates and thrust, the area of the throat was varied in the Propulsion Analysis Program as a function of flight time. This final simulation resulted in a calculated throat erosion that was considerably higher than predicted (Figure 1), but gave good matches to the measured data.

It is noted that the APS engine characterization equations (Reference 4) are not valid for this large an erosion rate. The specific impulse in the APS simulation is characterized partially as a function of the ratio of the initial throat area to the throat area at any time during the burn. Characterization limits on this ratio are 0.98 minimum to 1.03 maximum. The equations were modified in the Apollo Propulsion Analysis Program to extrapolate the specific impulse as a function of area of the throat beyond the upper limit of 1.03. The method of extrapolation (Figure 3) was to obtain normalized values of theoretical frozen and shifting equilibrium specific impulse (Isp) as a function of area of the throat (A_t). The slopes from these curves were used, as noted in Figure 3, to obtain the Isp as a function of A_t beyond Rocketdyne's characterization equation upper limit. The new characterization equation and throat erosion rate were then input to the Apollo Propulsion Analysis Program to simulate the large erosion rate. The method of establishing the erosion rate was to incorporate all APS flight data, including the Reaction Control System (RCS) thrust and flowrates and perform a best fit minimum variance solution, varying the area of the throat at each time slice to give the "best" correlation possible. Using this "best fit" solution, the flight data could be accurately simulated; without this greater erosion rate, the flight measurements could not be matched. In order to show the relationship between the engine chamber pressure, the differential pressures (tank bottom to engine interface) and the throat erosion, Figure 4 was compiled comparing the trends of these data. The trends were established based on the flight regulator performance with the predicted throat erosion rate and with the reconstructed erosion rate. The data in Figure 4 are the changes from the initial time slice of the steady-state analysis and are compared with the actual flight measurement changes. The data which incorporates the predicted low throat erosion does not match either the flight chamber pressure or the differential pressures as noted in Figure 4. Chamber pressure and oxidizer and fuel differential pressures match the flight data when incorporating the high throat erosion. It is noted that the larger throat area results in a greater decrease in chamber pressure and causes higher flowrates which give increasing differential pressures. Therefore, the large throat erosion was incorporated in the reconstruction and produced an excellent match to flight data as noted in Figures 5 through 10.

The APS throat erosion calculated by the above method was 5.3% during the BTD. This exceeds the maximum erosion exhibited during Rocketdyne altitude mission duty cycle tests, but only exceeds the 3σ dispersion (Reference 2) limit during the extreme latter portion of the burn. The effect of this larger erosion rate on future flight predictions would be to increase thrust levels and flowrates but decrease specific impulse. The overall effect of the increased erosion rate was to decrease burn time and create a minor degradation in performance (decreased Isp, increased thrust). During ground testing, Engine REA 0010A was subjected to a mission duty cycle similar to LM-3 (3-second firing followed by 45-minute altitude soak; another 3-second firing followed by a 4.5-hour altitude soak; then a final 342-second firing), and exhibited approximately 2-percent erosion compared to the 0.3 percent prediction. These two occurrences suggest that a short-duration firing, followed by an altitude soak and a long-duration firing, results in more severe throat erosion than a normal single long-duration firing. LM-4 flight data should provide additional evidence regarding this suspected phenomenon.

The engine interface pressures which were used in the simulation are presented in Figures 5 and 6. The measured pressures were 9 psia (oxidizer) and 8 psia (fuel) lower than predicted. In order to obtain satisfactory results, these interface pressures were statistically increased (biased) 1.3 psia, oxidizer, and 1.6 psia, fuel. Chamber pressure results are presented in Figure 10 and match the simulation incorporating the higher throat erosion with a slight drift in the measurement as a function of burn time. The tank bottom to interface differential pressures are represented in Figures 7 and 8. The simulation which includes the large throat erosion rate produced excellent residual values as previously noted. The RCS thrust used in the model is shown in Figure 11 and represents a curve fit of thrust data calculated from all on-off bilevel pulses throughout the BTD (Figure 12).

The effects of RCS thrust and flowrates on Lunar Module accelerations had to be determined in order to establish the APS performance. The RCS thrust and propellant consumption were calculated using thruster solenoid bilevel measurements. The "ON" time obtained from each solenoid was multiplied by the nominal thrust (100 lbf) and flowrates (0.24 lbm/sec oxidizer and 0.12 lbm/sec fuel) to obtain the thrust (Figure 12) and total consumption (Figures 13-15) for the period considered. During the APS burn to depletion (BTD), the RCS storage tanks provided propellants to RCS system "A". System "B" propellants were provided by the APS storage tanks. Propellant usage from the start of the APS propellant settling burn to APS BTD cutoff is shown in Table 5. The RCS thrust and flowrate data as calculated by the above method were characterized with 5th degree curve fits (as functions of time) and input to the APS Propulsion Analysis Program. These curve fits do not in general give the calculated instantaneous thrust and flowrates of Figures 12 through 15, but over the total time period evaluated they will give the same total impulse and mass change. It is noted that the level of the RCS simulated data could be in additional minor disagreement to actual flight data due to low APS engine interface pressures (helium regulator malfunction) and different performance levels due to RCS pulse durations. During the period of the BTD analyzed the RCS curve fit data gives satisfactory results.

APS thrust and oxidizer and fuel flowrates are presented in Figures 16, 17, and 18, respectively.

The acceleration residuals (measured minus calculated) are presented in Figure 9, and denote a good match over the 240 seconds of steady-state data which was analyzed. A measure of the quality of the match is given by the residual slope and intercept data shown in Figures 5 through 10. This data represents the intercept, on the ordinate, and slope of a linear fit to the residual data. It is readily seen that the closer both these numbers are to zero the better the match. All residuals as calculated in the minimum variance solution gave good slopes and intercepts as seen in Figures 5 through 10.

The actual APS burn time was observed to be less than the expected time calculated from engine flight data and propellant loading data. The oxidizer tank low-level sensor (LLS) was uncovered at approximately 101:59:02 GET, or at 347 seconds into the burn. The first indication of chamber pressure drop was at 101:59:07 GET, indicating oxidizer depletion. The oxidizer depletion was apparently 3 seconds premature based on the oxidizer tank LLS data and the reconstructed performance data. The analysis of Reference 7 indicated that propellant sloshing may have occurred and it could have been of such a magnitude as to have caused the three-second early cutoff. The effect of this sloshing would be equivalent to not burning 12 lbm of fuel and 20 lbm oxidizer. The allotment presently included in the CSM/LM Spacecraft Operational Data Book (Reference 8) is 7.1 lbm of fuel and 11.3 lbm of oxidizer, and is believed to be based on an erroneous zero "G" can height.

The fuel LLS was uncovered at approximately 101:59:12. Calculation of fuel mass consumed from the time of oxidizer LLS actuation to fuel LLS actuation indicated that there was approximately 105 lbm of fuel remaining at time of oxidizer LLS uncovering. Using this information along with the propellant available at BTD ignition (Table 4), and the calculated RCS interconnect usage during the BTD (Table 5), the average engine propellant mixture ratio (MR) was calculated to be 1.601 (.005 MR units less than predicted).

The preceding analysis indicates that the APS operated satisfactorily during the flight of Apollo 9. The following exceptions to nominal performance were noted:

1) The presently unexplained higher than predicted throat erosion.
2) The helium regulator malfunction.
3) The premature oxidizer depletion, due to propellant sloshing.

The APS BTD integrated average specific impulse and mixture ratio were 309.7 seconds and 1.601 MR units, respectively.

It is recommended that particular attention be given to the LM-4 throat erosion characteristics to determine if this erosion could possibly be a flight oriented phenomena.

Comparison with Preflight Performance Prediction

Predicted performance of the LM-3 APS is presented in Reference 2. The preflight report was intended to present the performance of LM-3 under predicted flight conditions. However, no attempt was made to simulate RCS operation and for that reason acceleration and velocity data presented in Reference 2 were qualified.

Table 6 presents a summary of actual and predicted APS performance during the BTD. Since the preflight prediction assumed a normally functioning regulator, there exists large differences between predicted and measured parameters, therefore, a reprediction was made based on the flight regulator performance in order to assess the adequacy of the flight prediction techniques and models. The measured flight data is seen to compare quite closely (Table 6) with the reconstructed parameters. Prelaunch checkout indicated an instrumentation bias on the flight regulator outlet pressure existed; this bias has been subtracted from the data presented in Table 6. Repredicted steady-state values and related three sigma dispersions for specific impulse, thrust and mixture ratio are presented in Figure 19. Corresponding data from the APS BTD analysis is also presented for purposes of comparison. The rise in the level of reconstructed thrust data is due to the increased throat erosion previously discussed. Variances seen in specific impulse data are also due to the higher throat erosion rate. The differences seen in mixture ratio data are due to a slight imbalance in propellant interface pressures. These variations lie within the three sigma dispersion limits throughout the span of data analyzed although it may be noted that the thrust would likely exceed the limits near the end of the BTD.

Engine Performance at Standard Inlet Conditions

Expected flight performance of the APS engine was based on a model characterized with data obtained during engine and injector acceptance tests.

In order to allow actual engine performance variations to be separated from performance variations induced by feed system, pressurization system and propellant temperature variations, the acceptance test data is adjusted to a set of standard inlet conditions, thereby providing a common basis for comparison. Standard inlet conditions are as follows:

Oxidizer interface pressure, psia	170.
Fuel interface pressure, psia	170.
Oxidizer interface temperature, °F	70.
Fuel interface temperature, °F	70.
Oxidizer density, lbm/ft^3	90.21
Fuel density, lbm/ft^3	56.39
Thrust acceleration, lbf/lbm	1.
Throat area, in^2	16.26

Analysis results (at 15 seconds from ignition) for the BTD corrected to standard inlet conditions and compared to acceptance test are as shown below:

	Acceptance Test Data	Flight Results	% Difference
Thrust, lbf	3509.	3480.	0.82%
Specific Impulse, $\frac{lbf\text{-}sec}{lbm}$	310.1	310.3	0.07%
Propellant Mixture Ratio	1.610	1.608	0.12%

These differences are well within the engine combined repeatability and acceptance instrumentation uncertainties. Flight interface pressures for that part of the BTD analyzed as steady-state were 6-8 psia below the predicted levels. As expected, reduced performance resulted from the lower in-flight interface pressures. However, adjusting engine performance to standard inlet conditions and comparing with acceptance test values show good agreement (all values within one sigma), therefore, indicating that the basic preflight prediction techniques are adequate with the possible exception of the throat erosion characterization. Review of this conclusion will be made based on future flight and ground test data.

PRESSURIZATION SYSTEM

Helium Utilization

The helium storage tanks were loaded to a nominal load of 13.1 lbm. The helium tank temperature and pressure at 175 hours before launch were 3,020 psia, 70° F and 2,988 psia, 70° F for tanks 1 and 2, respectively. There was no indication of helium leakage during the mission. Calculated helium usage during the burn agrees with analytical predictions. The pressure in the helium supply tanks during the BTD is presented in Figure 20.

Ullage Pressure Decay During Coast

The fuel and oxidizer interface pressures at launch were 172 and 158 psia, respectively. When the first data was received at 43:37 GET, the pressures had decayed to 167 and 148 psia. This pressure drop is attributed to the absorption of helium into the propellant; the pressure predicted for maximum helium solubility was 169 and 148 psia for fuel and oxidizer respectively.

Regulator Performance

Data received after the APS propellant pressurization and after the first APS burn indicated a regulator outlet pressure corresponding to that of the Class I primary helium regulator. However, during the second APS burn (BTD), measured regulator outlet pressure (Figure 21) was lower than expected (176 rather than 184 psia). These circumstances, i.e., that during a no-flow condition the regulator outlet pressure was nominal and that during flow it was lower than nominal indicates a flow restriction in the Class I leg of the regulator package. Regulation bands for the Class I and II primary and secondary regulators are shown in Figure 21. From Figure 21 it can be seen that regulator outlet pressure was within the band of the

Class II primary regulator for approximately the first 290 seconds of the BTD, at which time it shifted upward almost instantaneously, indicating that the Class I primary regulator had begun to control flow. White Sands Test Facility (WSTF) data on PA-1 (series 12, run 3, test 4 and series 8A, test 007) tends to substantiate this explanation (Reference 6). In addition, comparison of the depletion characteristics of the LM-3 regulator to WSTF tests show that both Class I and II regulators were flowing during depletion.

A solenoid located upstream of the Class I regulator was removed at KSC and during this operation it is possible that reverse flow through the regulator occurred. Such a reverse flow is considered to be a source of contamination and is the most probable cause of the regulator anomaly.

Reference 6 provides a detailed analysis of the regulator problem and arrives at the following conclusions:

1. The pilot poppet was sluggish at the beginning of the BTD.
2. The step-up in regulation pressure at 290 seconds into the burn is due to the Class I regulator starting to control flow.
3. Both Class I and Class II regulators were flowing at time of depletion.
4. Component testing of the regulator indicates that the forcing function in the pilot poppet is highly dependent upon sensing pressure, therefore, if the Class II regulator had not controlled flow at the 176 psi level the Class I would have been forced to flow prior to reaching the 120 psia redline.
5. The most probable cause of the LM-3 anomaly was contamination of the regulator during solenoid valve replacement.
6. The possibility of minor back-flowing exists in regulators through

LM-7. These regulators, however, have been functionally tested and operate within specification limit.

In view of the above conclusions Reference 6 states that the APS regulator design is considered to be adequate for the Apollo Program and that the question of the LM-3 anomaly is closed.

PROPELLANT LOADING AND USAGE PRIOR TO BURN TO DEPLETION

The oxidizer tank was fully loaded at a pressure of 66 psia and an oxidizer temperature of 71° F. The fuel tank was loaded at a pressure of 62 psia and a fuel temperature of 69° F. A density determination was made for both oxidizer (1.4816 GM/CC at 4° C and 14.7 psia) and fuel (.8998 GM/CC at 25° C and 14.7 psia) samples. Based on these density values, propellant tank pressures and temperatures, a determination was made on the quantity of propellant to off load. This off load (430.9 lbm fuel and 752.1 lbm oxidizer) was performed, using the weigh tank three times. The actual propellant load was determined to be 1626.2 lbm fuel and 2523.9 lbm oxidizer.

APS propellant usage prior to the BTD, both by the APS and by the RCS through the APS/RCS interconnect, is presented in Table 4. The APS propellant load at APS BTD ignition is estimated to have been 1592 lbm fuel and 2461 lbm oxidizer.

ENGINE TRANSIENT ANALYSIS

An analysis of the start and shutdown transients was performed to determine the transient total impulse, and to characterize the engine when operating in an oxidizer depletion shutdown mode. The results of this analysis are summarized in Table 7. Engine acceptance test data specification requirements as well as ground test data were used in the analysis of the flight test results.

In general, all applicable transient specification requirements have been satisfied and a favorable comparison of flight data with ground test data was obtained. Representative traces of the start and shutdown transients are presented in Figures 22 and 23.

A more detailed discussion of the pertinent engine transient characteristics are presented below.

Start Transient

The information presented in Table 7 provides a comparison of the engine start transient data. The time from engine-on signal (FS-1) to 90 percent steady-state thrust was 0.221 seconds for the second burn and was on an average of 75 ms faster than engine acceptance test data. The faster start transient time is primarily due to the second start being conducted with a primed fuel actuator line whereas the acceptance tests were conducted with a dry actuator line. From data acquired during the engine qualification program it was determined that primed starts were characteristically in the order of 100 ms faster than unprimed starts. From inspection of the flight data, it was also apparent that the valve actuation time was slightly faster than experienced during the engine acceptance tests.

Consequently, as the result of a faster valve actuation time and a primed start, the start transient impulse was lower than that determined during engine acceptance testing. However, it should be noted that the start transient time and impulse meet the required specification criteria.

As noted in Table 7, the maximum chamber pressure overshoot value met the specification requirement. However, it should be stated that no ground tests have been conducted with flight chamber pressure instrumentation installed in the flight configuration and tested on vehicle configured test stands. Therefore, no ground test data is available to determine whether the chamber pressure overshoot was attenuated or amplified with the flight configured instrumentation installation. However, test data is available from specially instrumented start-shutdown characterization tests, conducted at the engine contractor's facility and at the WSTF PA-1 test stand that indicate the measured over-shoot value is reasonably accurate and representative of the actual chamber pressure overshoot. The engine start transient characteristic is presented in Figure 22. There was no evidence of footballs, low frequency oscillations, ignition spikes or pre-priming pulses during the start transient.

Shutdown Transient

The transient characteristics that the engine demonstrated during an oxidizer depletion shutdown mode are shown in Figure 23. The data presented in Table 7 provides comparison of flight data to ground test data obtained from the WSTF PA-1-8A-006B run. The data indicate that the characteristics of the oxidizer depletion agreed favorably with the ground test conducted at WSTF. No detrimental effects or hazardous behavior such as shutdown spikes or pops were observed during the oxidizer depletion shutdown mode.

REFERENCES

1. TRW IOC 69.4354.2-29, "LM-3 APS preliminary Postflight Analysis," from P. F. Thompson to D. W. Vernon, dated 10 April 1969.

2. NASA memorandum, "Revised APS Mission D Preflight Analyses and Review of Mission D Preflight Analyses for SPS and LM," J. G. Thibodaux, Jr., dated 30 December 1968.

3. Rocketdyne Engine Log Book, "Acceptance Test Data Package for Rocket Engine Assembly - Ascent LM- Part No. RS000390-001-01, Serial No. 0004," dated 21 August 1968.

4. North American Rockwell Corporation Document No. PAR 8114-4102, "Lunar Module Ascent Engine Performance Characterization," prepared by T. A. Clemmer, dated 10 July 1968.

5. NASA/MSC Report MSC-PA-R-69-2, "Apollo 9 Mission Report," dated May 1969.

6. NASA Memorandum, "Assessment of LM-3 APS Regulator Anomaly," C. E. Humphries, dated 28 May 1969.

7. Telecon with J. Protopapas, Grumman Aircraft Engineering Corporation, June, 1969.

8. NASA/MSC SNA-8-D-027(III), Rev. I, "CSM/LM Spacecraft Operational Data Book, Vol. III, Rev. 1," dated November 1969.

TABLE 1 - LM-3 APS DUTY CYCLES

BURN	Ignition FS-1 Hr:min:sec GET	Engine Cutoff FS-2 Hr:min:sec GET	Burn Duration Seconds	Velocity(1) Change ft/sec
APS 1st Burn Constant Delta Height Maneuver	96:58:15	96:58:17.9	2.9	42.4
APS 2nd Burn Burn to Depletion	101:53:15.4	101:59:17.7	362.3	5373.4

(1)Reference 5

TABLE 2

LM-3 APS ENGINE AND FEED SYSTEM PHYSICAL CHARACTERISTICS

Engine[1]	
Engine No.	Rocketdyne S/N 0004B
Injector No.	Rocketdyne S/N 4097706
Initial Chamber Throat Area (in^2)	16.117
Nozzle Exit Area (in^2)	748.50
Initial Expansion Ratio	46.44
Injector Resistance (lb_f-sec^2/lb_m-ft^5) @ Time Zero and 70°F	
Oxidizer	12583.
Fuel	20472.
Feed System[2]	
Resistance, Tank Bottom to Engine Interface (lb_f-sec^2/lb_m-ft^5) at 70°F	
Oxidizer	2632.1
Fuel	4132.7

[1] Reference 1

[2] Per telecon with L. Rothenberg of GAEC.

TABLE 3

FLIGHT DATA USED IN STEADY STATE ANALYSIS

Measurement Number	Description	Range	Sample Rate Sample/Sec
GP2010P	Pressure, Thrust Chamber	0-150 psia	100
GP1503P	Pressure, Engine Oxidizer Interface	0-250 psia	1
GP1501P	Pressure, Engine Fuel Interface	0-250 psia	1
GP1116P	Pressure Difference, Oxidizer Tank Bottom to Interface	0-35 psia	10
GP0616P	Pressure Difference, Fuel Tank Bottom to Interface	0-35 psia	10
GP1408X	Oxidizer Tank Low Level Sensor	Off - On	1
GP0025P	Pressure, Regulator Outlet Manifold	0 - 300 psia	1
GP1218T	Temperature, Oxidizer Tank Bulk	20 - 120°F	1
GP0718T	Temperature, Fuel Tank Bulk	20 - 120°F	1

TABLE 4 - PROPELLANT USAGE FROM ASCENT PROPULSION SYSTEM
PRIOR TO BURN TO DEPLETION

Event	Time, hr:min:sec	Used (lbm)		Remaining (lbm)	
		Oxidizer	Fuel	Oxidizer	Fuel
Launch	0:00:00	--	--	2524	1626
Coelliptic sequence initiate maneuver (reaction control usage through interconnect) - estimated; no data available	96:16:03	20	10	2504	1616
Constant delta height maneuver (first ascent engine firing) - usage estimated; no data available	96:58:14	26	16	2478	1600
Ullage-settling plus X translation with reaction control system through interconnect	101:52:42	17	8	2461	1592
Ignition for ascent propulsion firing to depletion	101:53:15	--	--	2461	1592

TABLE 5

RCS PROPELLANT USAGE DURING APS BTD

	RCS Storage Tanks (lbm)			APS Storage Tanks (lbm)		
	Oxidizer	Fuel	Total	Oxidizer	Fuel	Total
Propellant Settling	0	0	0	16.9	8.5	25.4
APS (BTD) Ignition* to Depletion	52.7	26.3	79.0	28.9	14.5	43.4
TOTALS	52.7	26.3	79.0	45.8	23.0	68.8

*This RCS data table was derived from RCS thruster measurements GH1423V and GH1427V. These values represent approximately 99% of RCS activity with the exception of a 10-second data blackout during the APS BTD.

TABLE 6 - STEADY-STATE PERFORMANCE DURING BURN TO DEPLETION

PARAMETER	15 Sec after Ignition				150 Sec after Ignition				340 Sec after Ignition (d)			
	Predicted		Reconstruction(b)	Measured(c)	Predicted		Reconstructed(b)	Measured(c)	Predicted		Reconstruction(b)	Measured(c)
	(a)	(e)			(a)	(e)			(a)	(e)		
Regulator Outlet Pressure (psia)	186	178	178	178	185	177	177	177	185	180	180	180
Oxidizer Bulk Temperature °F	68	68	68	68	68	68	68	68	67	67	68	68
Fuel Bulk Temperature °F	68	68	68	68	68	68	68	68	68	68	68	68
Oxidizer Interface Pressure, psia	172	164	164	164	171	163	164	164	169	166	166	165
Fuel Interface Pressure, psia	172	164	164	162	171	163	164	162	170	161	166	165
Engine Chamber Pressure, psia	125	120	120	120	124	119	119	119	123	121	119	119
Mixture Ratio	1.609	1.606	1.604	--	1.606	1.603	1.599	--	1.601	1.599	1.599	--
Thrust, lb	3508	3382	3370	--	3481	3338	3390	--	3471	3396	3484	--
Specific Impulse, sec	310.1	310.1	310.3	--	310.3	310.3	309.8	--	309.6	309.6	308.9	--

(a) Preflight prediction based on acceptance test data and assuming nominal system performance.
(b) Reconstruction, minimum variance technique.
(c) Actual flight data with known biases removed.
(d) Data for this time slice not considered for steady-state analysis.
(e) Reprediction based on flight regulator outlet data.

TABLE 7 ASCENT ENGINE TRANSIENT ANALYSIS

Parameter	LM-3 ascent engine firings						White Sands test results	Class nominal values	Specification values
	Second inflight firing	Engine acceptance tests							
		First	Second	Third	Fourth	Average			
Time from ignition signal to initial thrust rise, sec	0.146	0.280	0.270	0.275	0.200	0.256	0.145		
Time from ignition signal to 90 percent of steady-state thrust, sec	0.221	0.320	0.296	0.307	0.264	0.297	0.256	0.265 - 0.351	[a,b]0.360 max.
Time from indicated beginning of valve opening to full open, sec	0.090	0.116	0.115	0.115	0.090	0.109	0.128		
Maximum value of chamber pressure overshoot during start, psia	178								[a]178 max.
Start transient total impulse from ignition signal to 90 percent steady-state thrust, lb-sec	≈25	61.4	56.0	51.1	56.1	56.2	≈35.4	35 - 61	[b]10 - 80
Engine run-to-run repeatability, lb-sec						±5.1		±13	[a]±35
Time from indicated chamber pressure decay to cutoff signal, sec	11						10		
Maximum peak-to-peak chamber pressure oscillation during shutdown, psia	35						23		
Chamber pressure decay rate from steady-state to cutoff signal, psia/sec	10						11.6		
Chamber pressure at cutoff signal, psia	9						8		
Shutdown transient impulse from steady-state thrust, sec	≈14 623						≈13 230		
Nominal shutdown transient impulse from cutoff signal to 10 percent steady-state thrust, lb-sec	*	364.2	337.3	350.6	319.6	342.9		231 - 367	[b]240 - 390
Engine run-to-run shutdown repeatability, lb-sec						±23.3		±73	[a]±75

[a]Contractor's engine design requirement specification.

[b]Vendor's acceptance test specification.

*Not applicable

FOLDOUT FRAME 1

FOLDOUT FRAME

FOLDOUT FRAME

FOLDOUT FRAME 2

APOLLO 9 SC104/LM3-APS-(RAW DATA),PCM,BURN 2,TEX/64

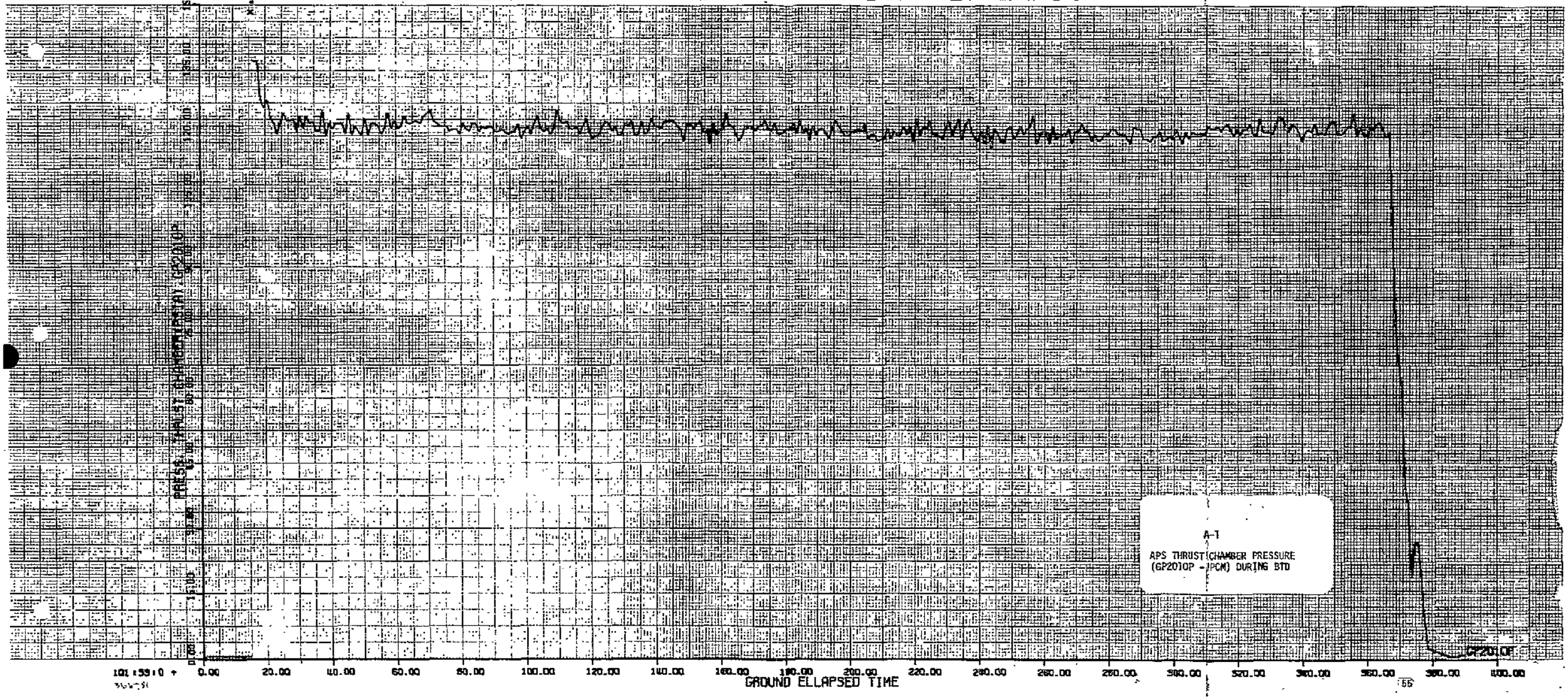

A-1
APS THRUST CHAMBER PRESSURE (GP2010P - PCM) DURING BTD

FOLDOUT FRAME 1

FOLDOUT FRAME 2

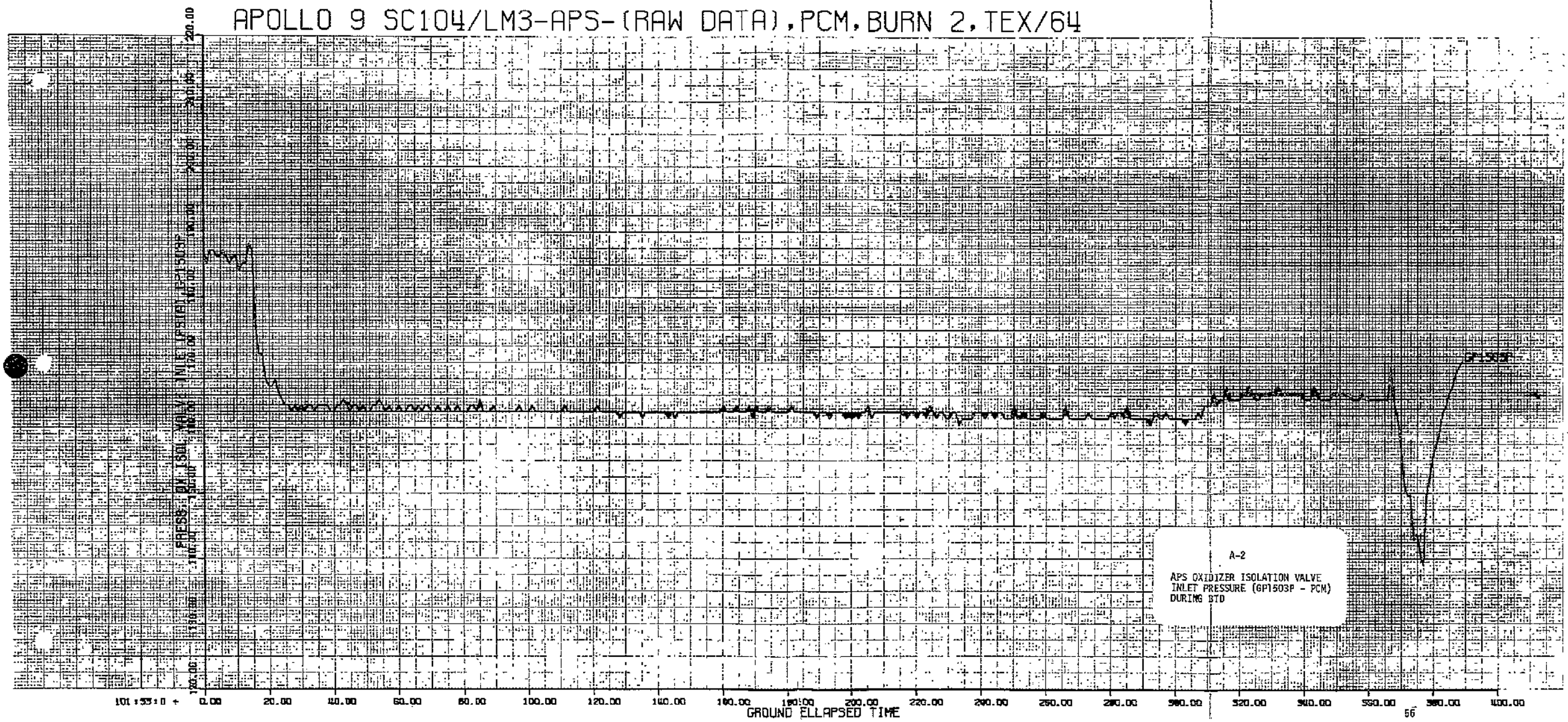

A-2

APS OXIDIZER ISOLATION VALVE INLET PRESSURE (GP1503P - PCM) DURING BTD

FOLDOUT FRAME 1

FOLDOUT FRAME 2

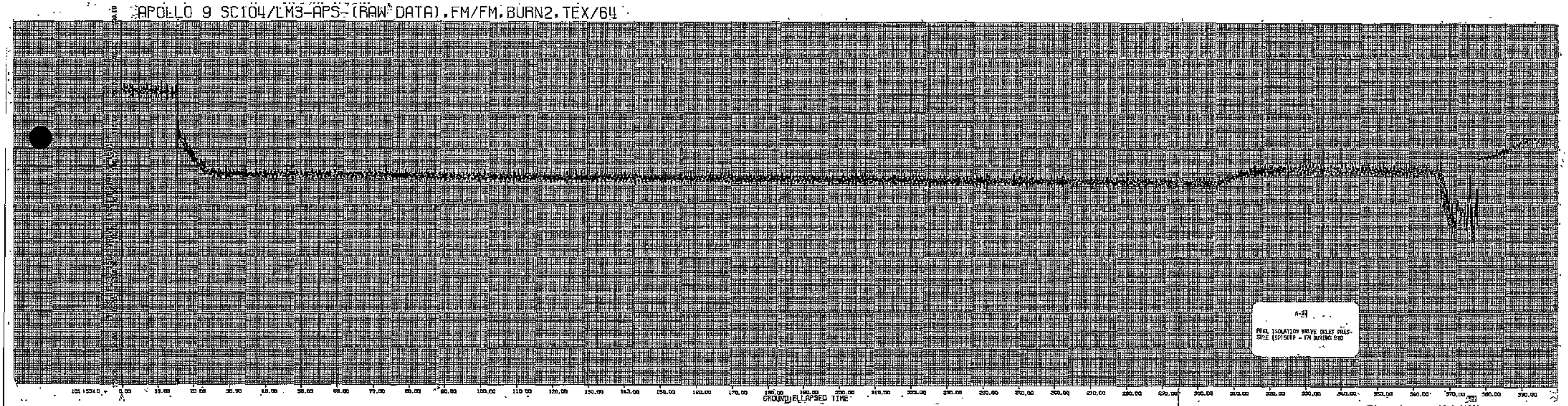

A-21

FUEL ISOLATION VALVE INLET PRESSURE (SP1501P - FM DURING BTD

FOLDOUT FRAME 1

FOLDOUT FRAME 2

FOLDOUT FRAME 2

APOLLO 9 SC104/LM3-APS-(RAW DATA),PCM,BURN 2,TEX/64

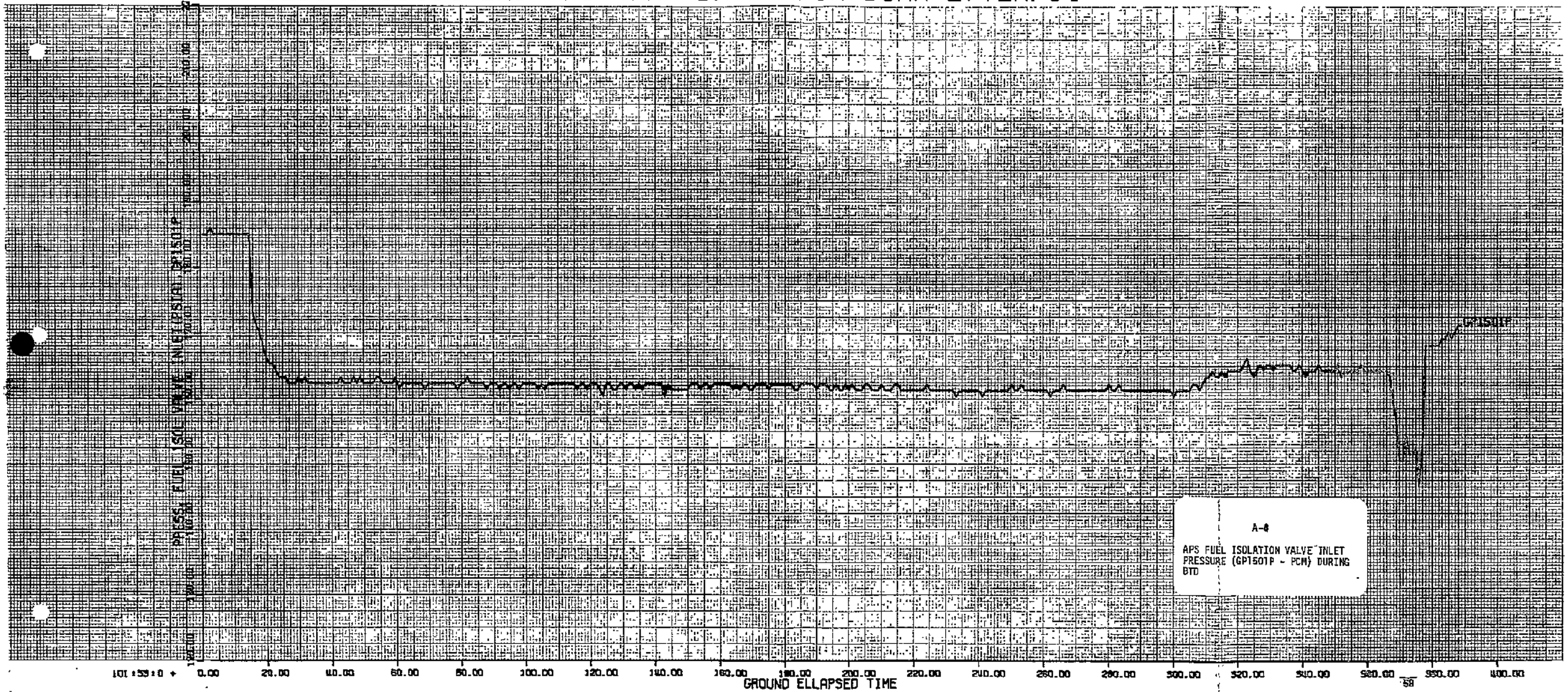

A-8

APS FUEL ISOLATION VALVE INLET PRESSURE (GP1501P - PCM) DURING BTD

FOLDOUT FRAME 1

FOLDOUT FRAME 2

FOLDOUT FRAME 2

APOLLO 9 SC104/LM3-APS-(RAW DATA),PCM,BURN 2,TEX/64

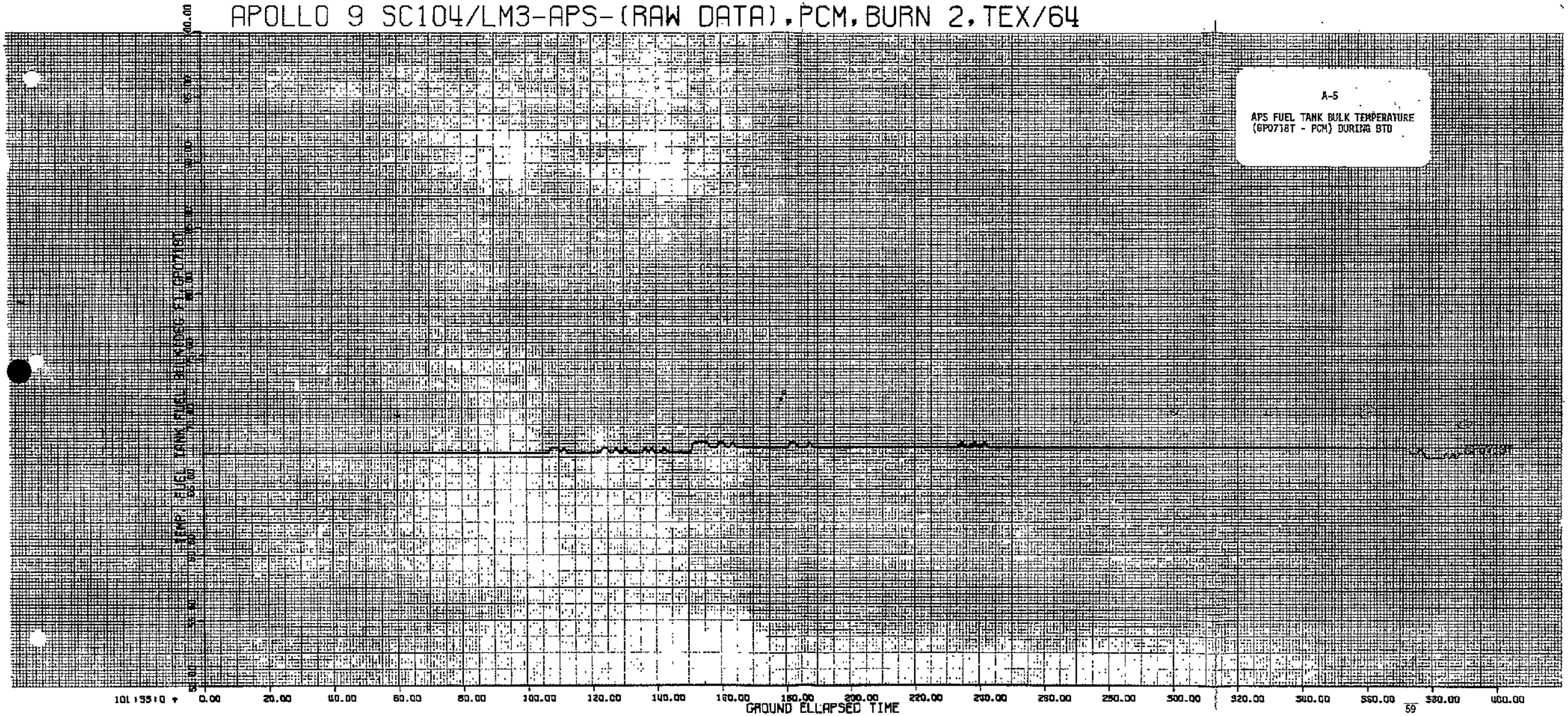

FOLDOUT FRAME 1

FOLDOUT FRAME 2

FOLDOUT FRAME 2

APOLLO 9 SC104/LM3-APS-(RAW DATA),PCM,BURN 2,TEX/64

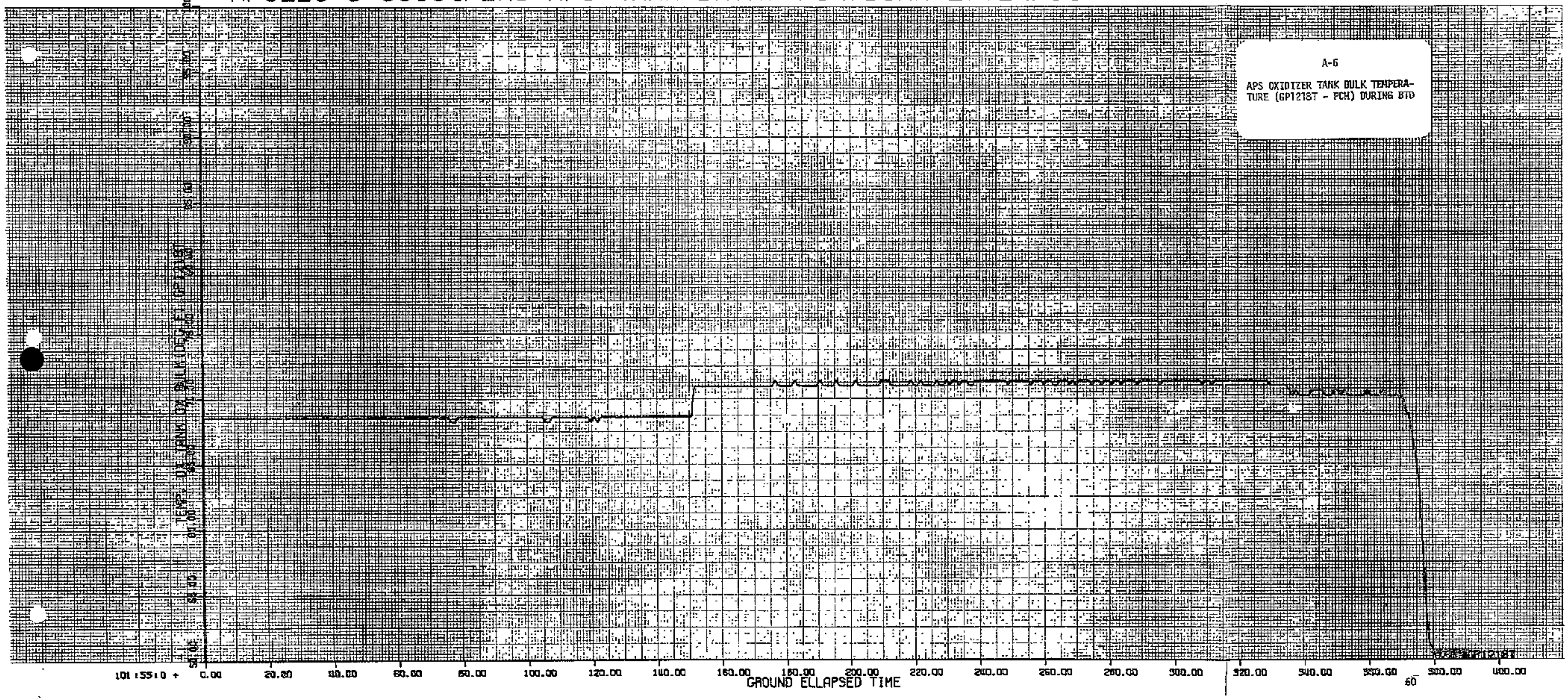

A-6

APS OXIDIZER TANK BULK TEMPERATURE (GP1218T - PCM) DURING BTD

FOLDOUT FRAME 1

FOLDOUT FRAME 2

FOLDOUT FRAME 2

APOLLO 9 SC104/LM3-APS-(RAW DATA),PCM,BURN 2,TEX/64

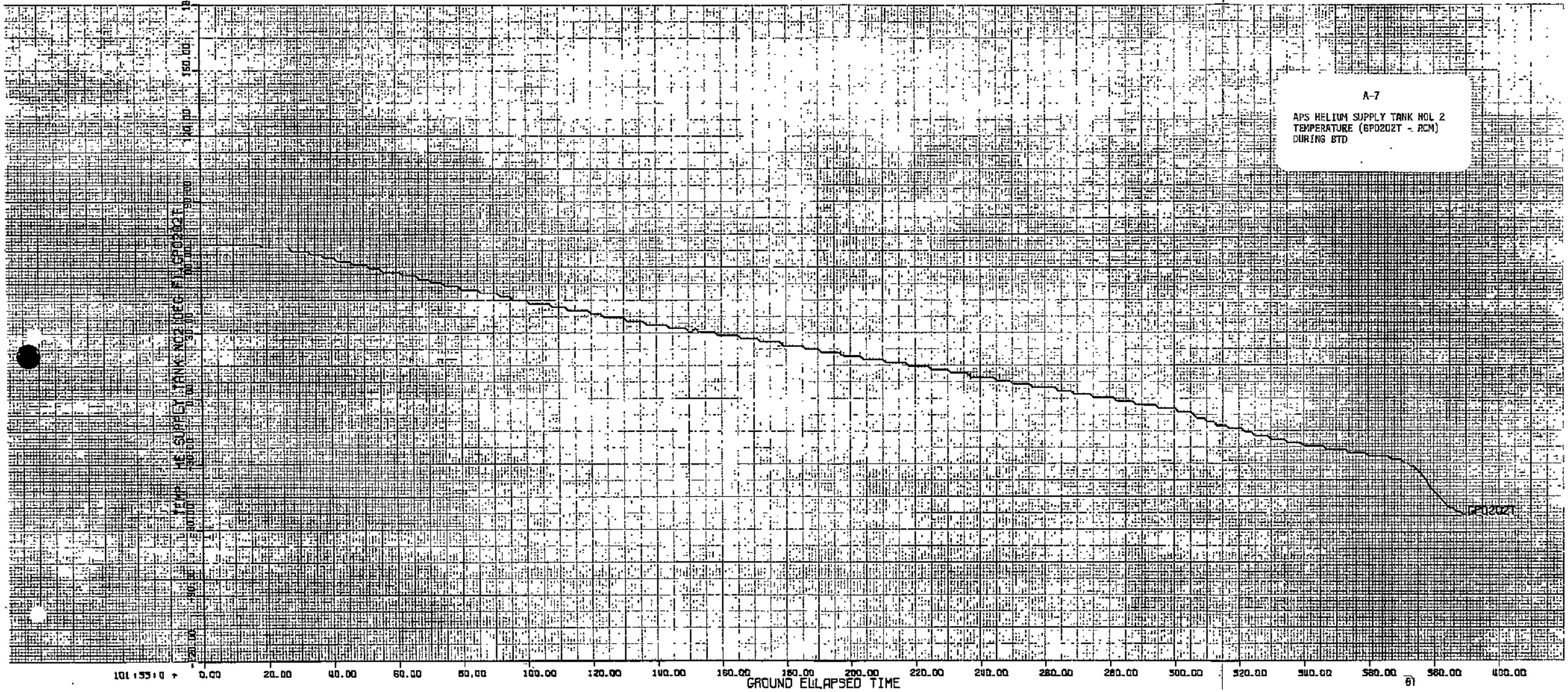

FOLDOUT FRAME 1

FOLDOUT FRAME 2

FOLDOUT FRAME 2

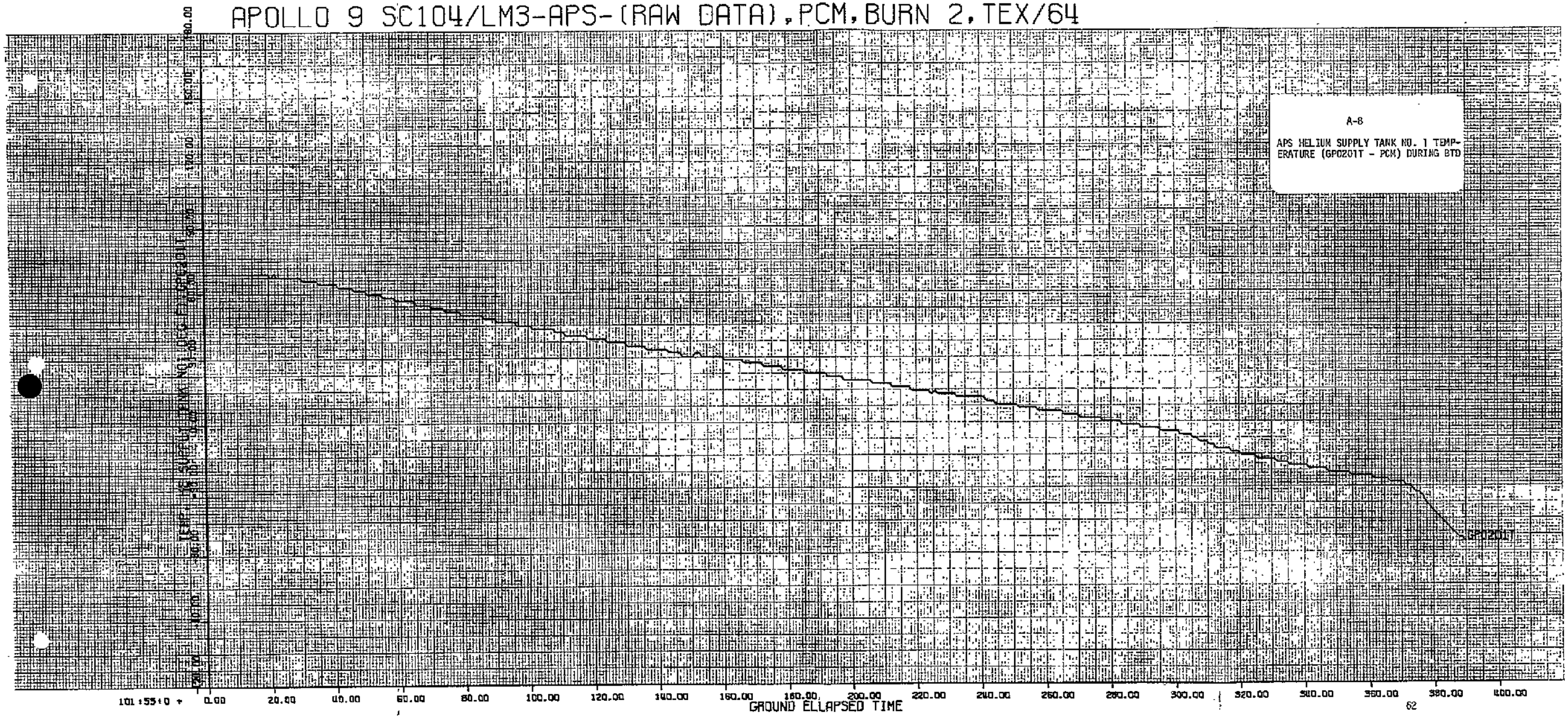

FOLDOUT FRAME 1

FOLDOUT FRAME 2

FOLDOUT FRAME 2

APOLLO 9 SC104/LM3-APS-(RAW DATA),PCM,BURN 2,TEX/64

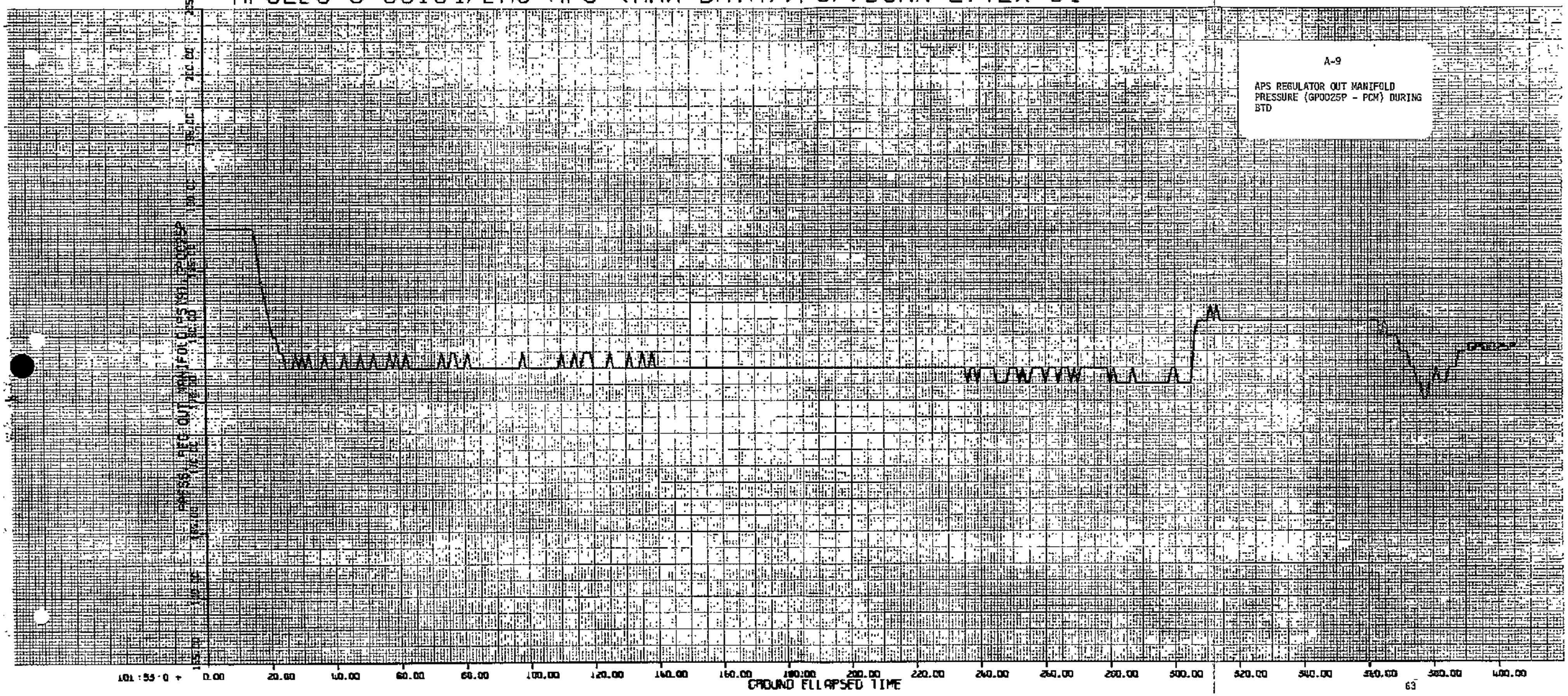

FOLDOUT FRAME 1

FOLDOUT FRAME 2

FOLDOUT FRAME 2

APOLLO 9 SC104/LM3-APS-(RAW DATA),PCM,BURN 2,TEX/64

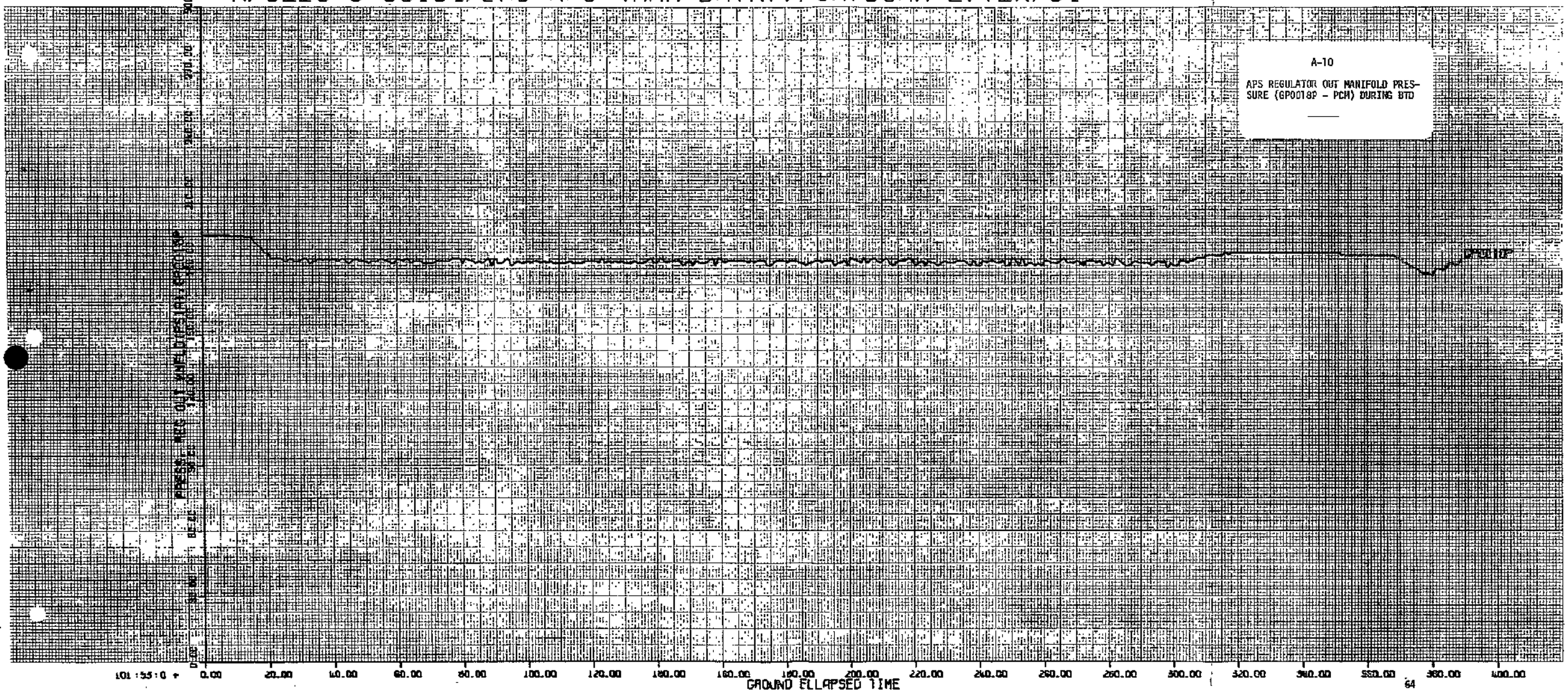

A-10

APS REGULATOR OUT MANIFOLD PRESSURE (GP0018P - PCM) DURING BTD

FOLDOUT FRAME 1

FOLDOUT FRAME 2

FOLDOUT FRAME 2

APOLLO 9 SC104/LM3-APS-(RAW DATA),PCM,BURN 2,TEX/64

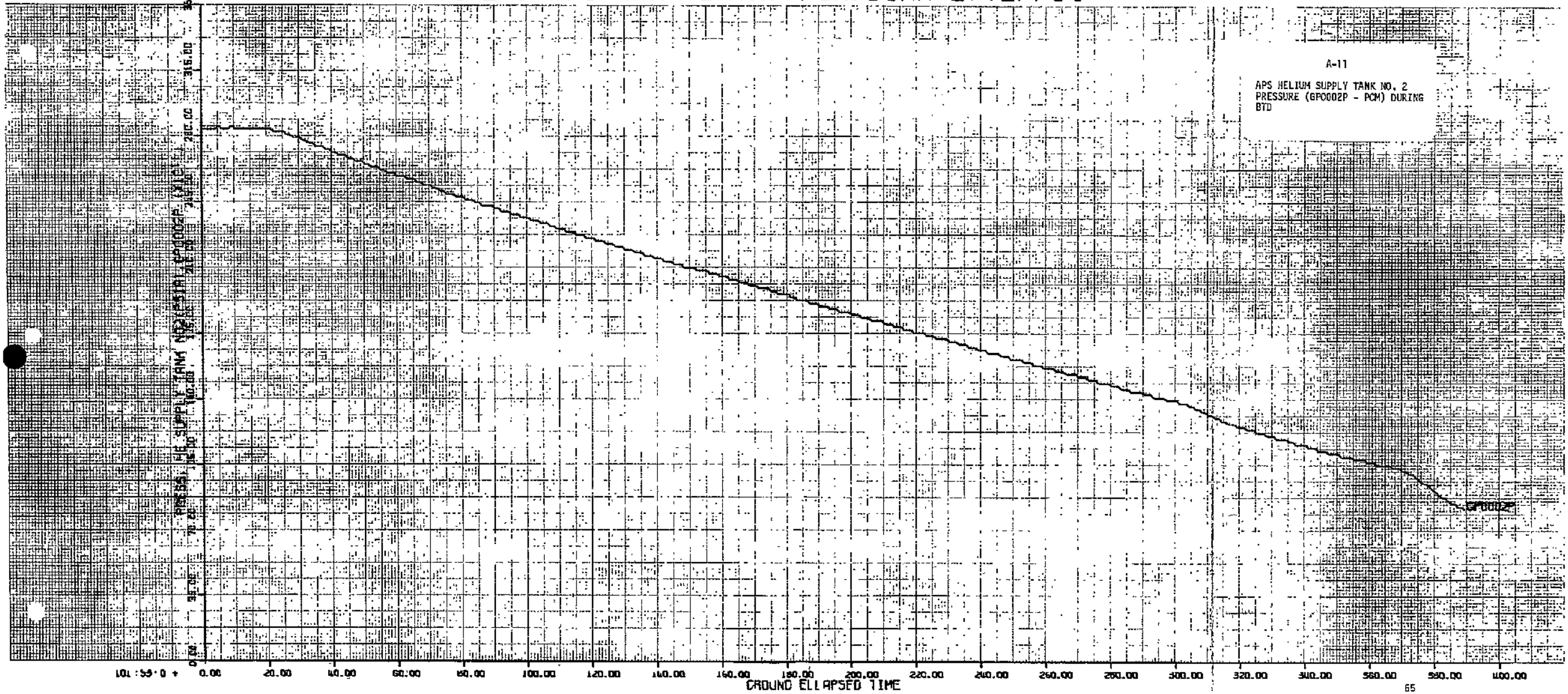

A-11

APS HELIUM SUPPLY TANK NO. 2 PRESSURE (GP0002P - PCM) DURING BTD

FOLDOUT FRAME 1

FOLDOUT FRAME 2

FOLDOUT FRAME 2.

APOLLO 9 SC104/LM3-APS-(RAW DATA),PCM,BURN 2,TEX/64

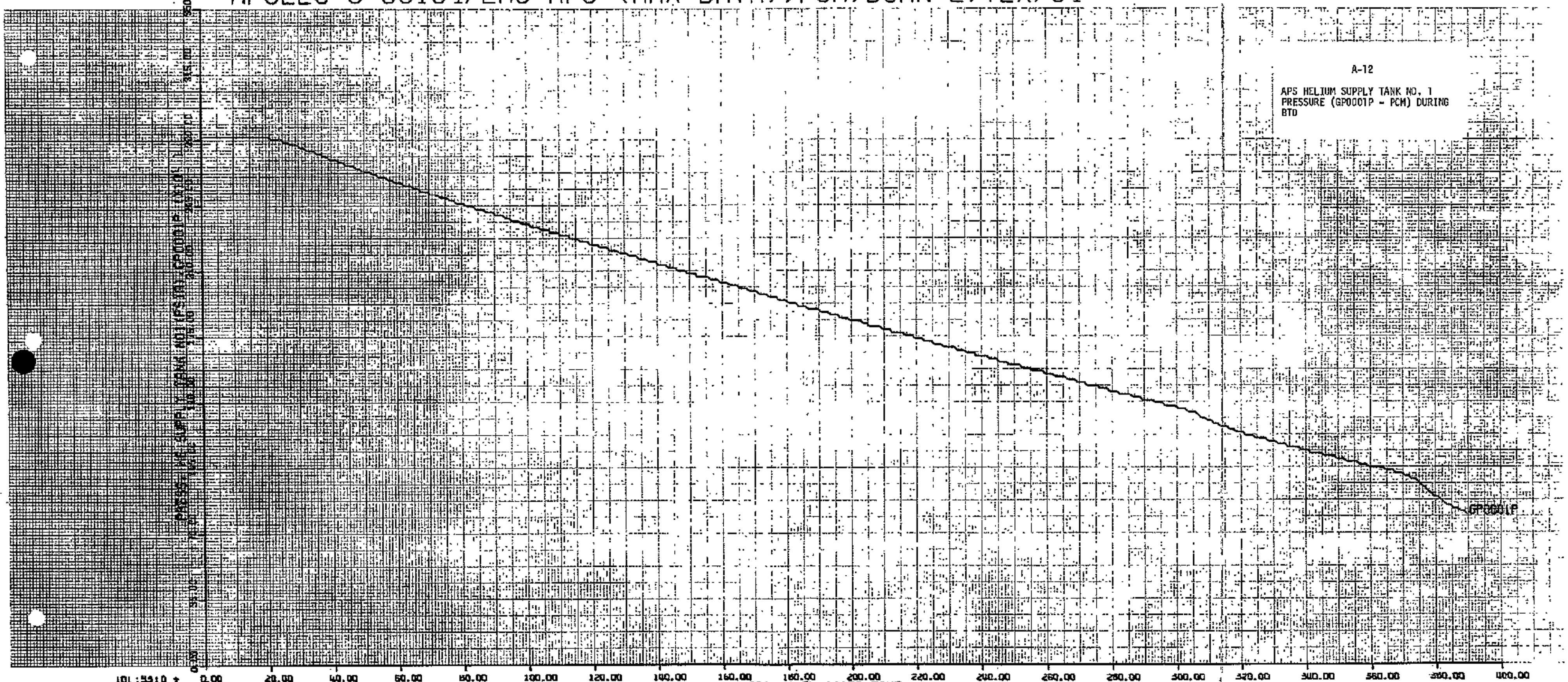

A-12

APS HELIUM SUPPLY TANK NO. 1 PRESSURE (GP0001P - PCM) DURING BTD

FOLDOUT FRAME 1

FOLDOUT FRAME 2

FOLDOUT FRAME 2

APOLLO 9 SC104/LM3-APS-(RAW DATA),PAM,BURN2,TEX/64

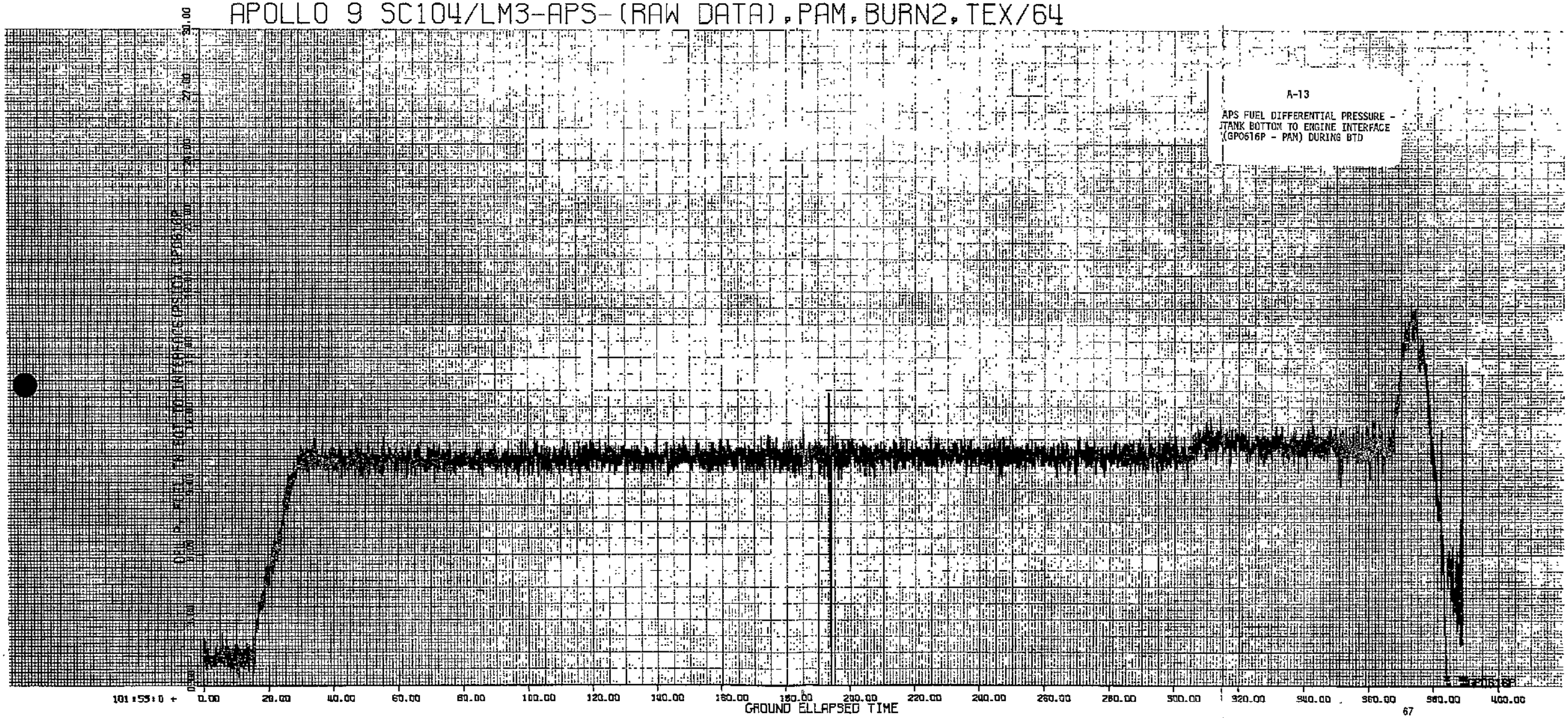

A-13

APS FUEL DIFFERENTIAL PRESSURE - TANK BOTTOM TO ENGINE INTERFACE (GP0616P - PAM) DURING BTD

FOLDOUT FRAME 1

FOLDOUT FRAME 2

FOLDOUT FRAME 2

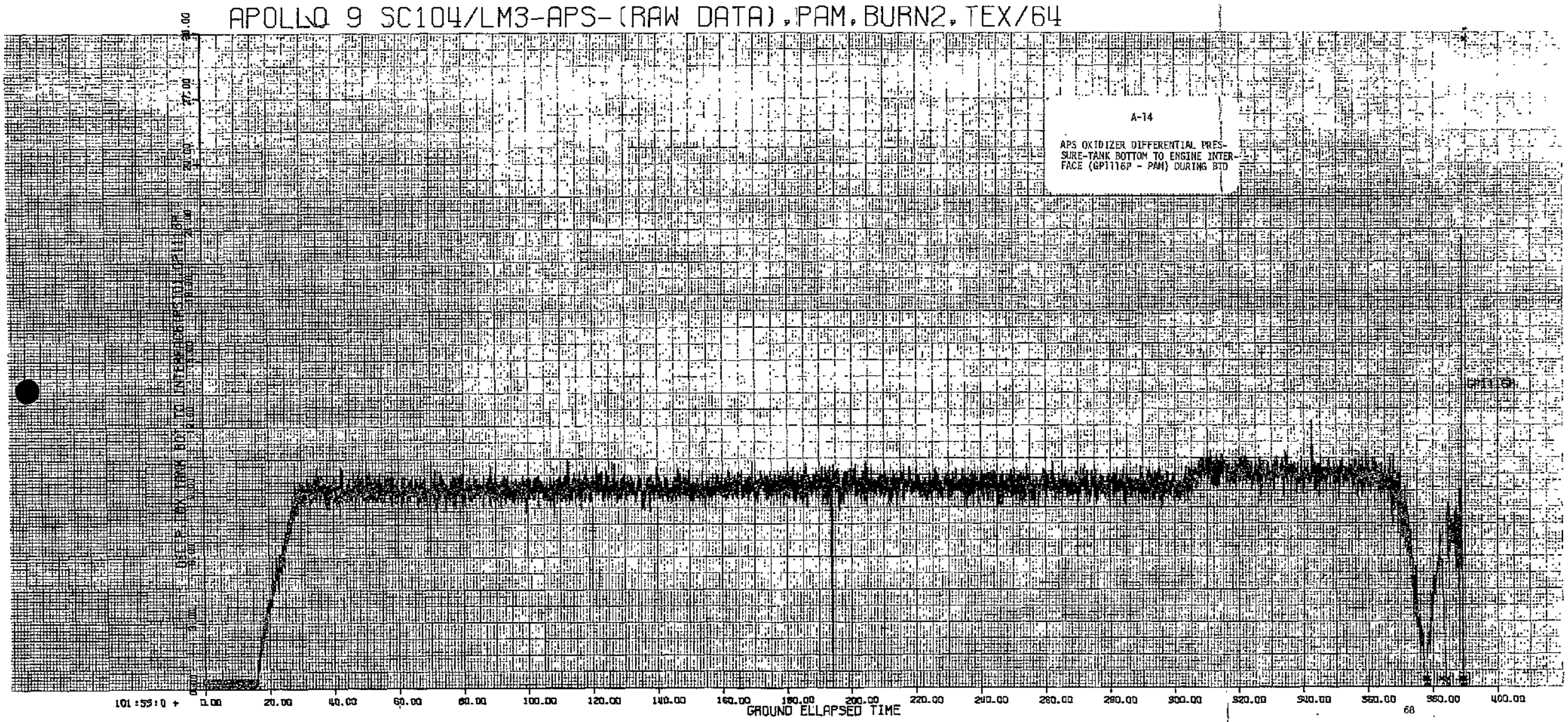

A-14

APS OXIDIZER DIFFERENTIAL PRESSURE-TANK BOTTOM TO ENGINE INTERFACE (GP1116P - PAM) DURING BTD

FOLDOUT FRAME 1

FOLDOUT FRAME 2

FOLDOUT FRAME 2

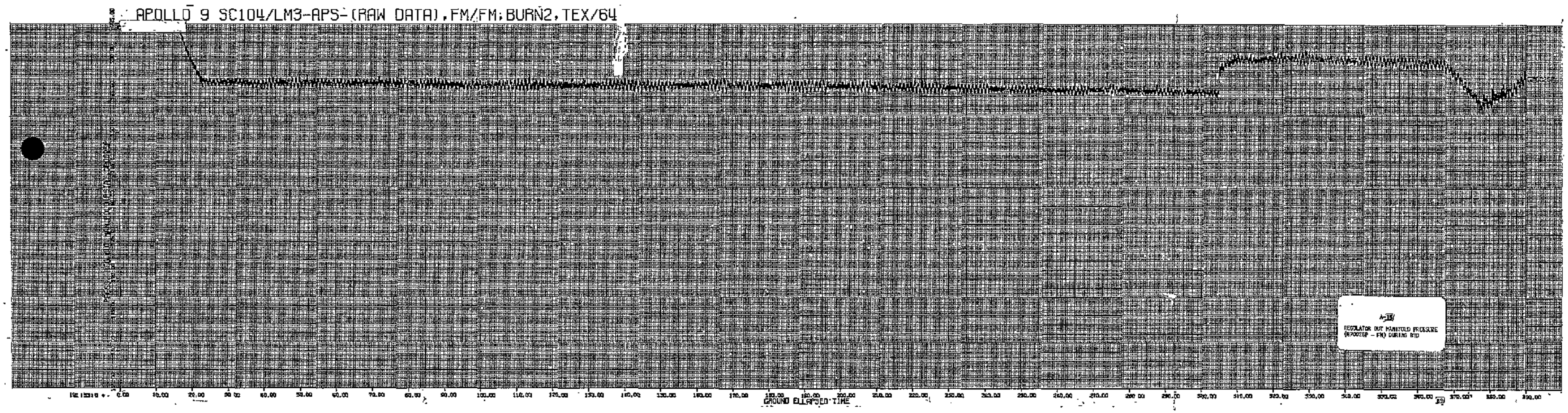

FOLDOUT FRAME 1

FOLDOUT FRAME 2

FOLDOUT FRAME 2

APOLLO 9 SC104/LM3-APS (RAW DATA),FM/FM,BURN2,TEX/64

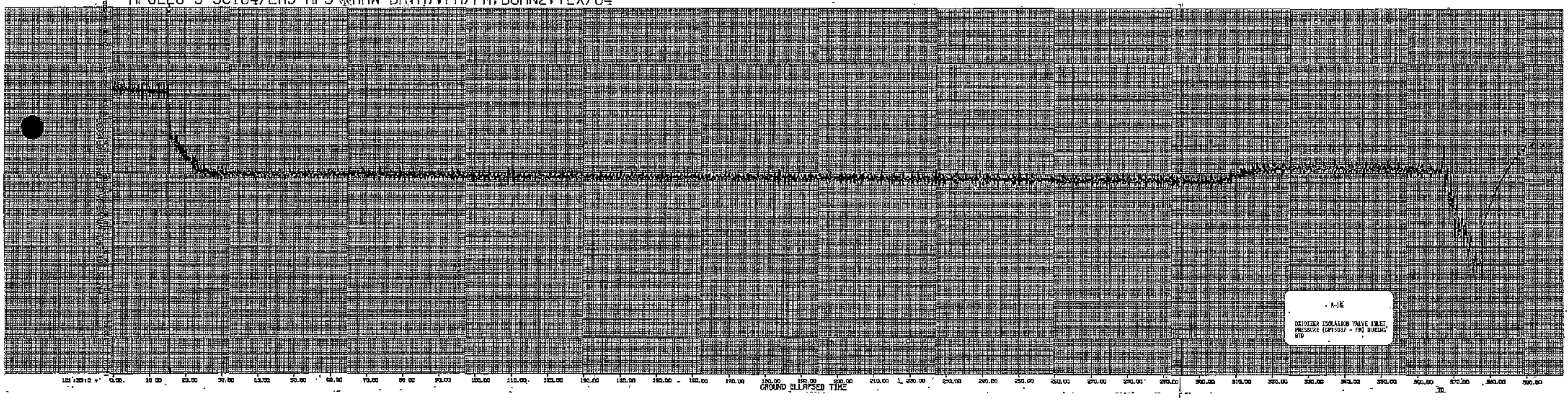

FOLDOUT FRAME 1

FOLDOUT FRAME 2

FOLDOUT FRAME 2

APOLLO 9 SC104/LM3-APS-(RAW DATA),FM/FM,BURN2,TEX/64

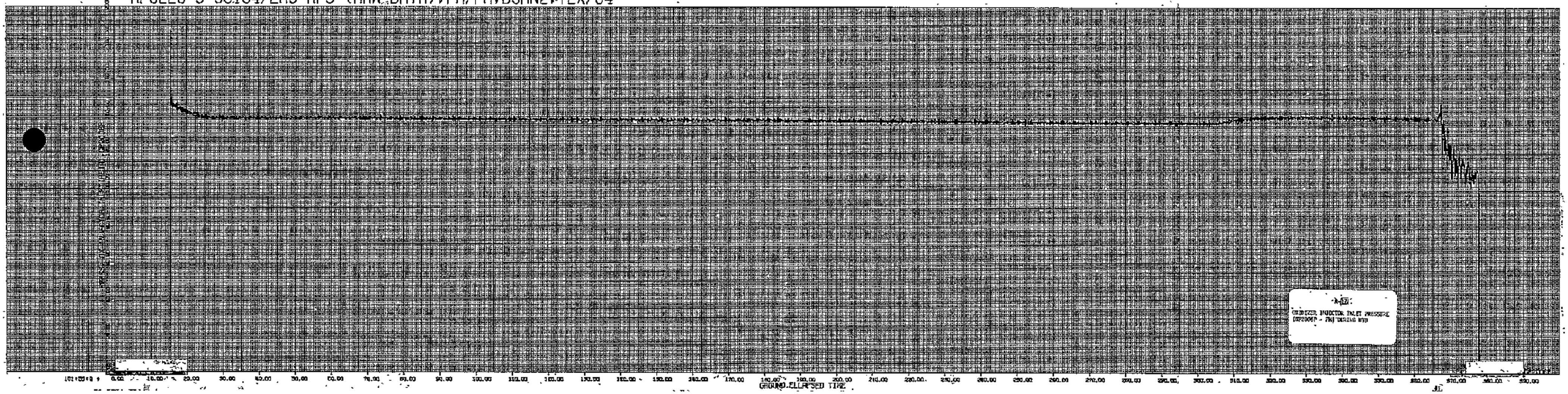

FOLDOUT FRAME 1

FOLDOUT FRAME 2

FOLDOUT FRAME 2

APOLLO 9 SC104/LM3-APS-(RAW DATA).FM/FM,BURN2,TEX/64